Assessment of the PM2.5 oxidative potential in a coastal industrial city in Northern France: Relationships with chemical composition, local emissions and long range sources

Lamia Moufarrej, Dominique Courcot, Frédéric Ledoux

▶ **To cite this version:**

Lamia Moufarrej, Dominique Courcot, Frédéric Ledoux. Assessment of the PM2.5 oxidative potential in a coastal industrial city in Northern France: Relationships with chemical composition, local emissions and long range sources. Science of the Total Environment, 2020, 748, pp.141448. 10.1016/j.scitotenv.2020.141448 . hal-03491412

HAL Id: hal-03491412
https://hal.science/hal-03491412

Submitted on 22 Aug 2022

HAL is a multi-disciplinary open access archive for the deposit and dissemination of scientific research documents, whether they are published or not. The documents may come from teaching and research institutions in France or abroad, or from public or private research centers.

L'archive ouverte pluridisciplinaire **HAL**, est destinée au dépôt et à la diffusion de documents scientifiques de niveau recherche, publiés ou non, émanant des établissements d'enseignement et de recherche français ou étrangers, des laboratoires publics ou privés.

Distributed under a Creative Commons Attribution - NonCommercial 4.0 International License

Version of Record: https://www.sciencedirect.com/science/article/pii/S0048969720349779
Manuscript_04626809339d8dc7099abf74d1e0b8e1

Assessment of the $PM_{2.5}$ oxidative potential in a coastal industrial city in Northern France: relationships with chemical composition, local emissions and long range sources

Lamia MOUFARREJ, Dominique COURCOT and Frédéric LEDOUX*

Unité de Chimie Environnementale et Interactions sur le Vivant, UCEIV UR4492, SFR Condorcet FR CNRS 3417, Univ. Littoral Côte d'Opale, 145 avenue Maurice Schumann, 59140 Dunkerque, France

*corresponding author: frederic.ledoux@univ-littoral.fr

Abstract

The objective of this work was to relate $PM_{2.5}$ Oxidative Potential (OP) data to PM composition and PM local and distant source contributions. $PM_{2.5}$ collected in Dunkerque, a coastal industrial city in North of France, was extensively characterized for major and minor chemical species. $PM_{2.5}$ filters were extracted using a synthetic pulmonary fluid to achieve OP estimation based on Ascorbic Acid (AA) and dithiothreitol (DTT) depletion assays. In order to evidence relationships between OP values, chemical composition and local and distant source contributions, correlation coefficient, Principal Component Analysis (PCA), concentration roses and polar plots and concentration weighted trajectories were used. Heterogeneous conclusions were drawn using the three first methods as the bivariate polar plots lead to dismiss some of the correlation evidenced using correlation coefficient and PCA. Both AA and DTT tests appeared complementary as they were not sensitive to the same species/source contribution. The bivariate polar plot representation of OP values versus wind direction and wind speed revealed that $PM_{2.5}$ concentration and combustion sources were linked to OP-AA, whereas emissions from integrated steelworks, electric steelworks, heavy

© 2020 published by Elsevier. This manuscript is made available under the CC BY NC user license
https://creativecommons.org/licenses/by-nc/4.0/

fuel oil combustion and traffic non-exhaust significantly contribute to OP-DTT.Sea-salts, aged sea-salts, crustal, secondary sulfates and secondary nitrates sources were not found to contribute to OP values. Constant weighted trajectories evidenced several source regions responsible for high OP values with Belgium, Germany and Netherland at the leader position. Contribution of inland regions appeared possibly related to the biomass and traffic related combustion while heavy fuel oil combustion could be also involved in the contribution of marine and coastal areas.

Keywords: $PM_{2.5}$; source contribution; oxidative potential; dithiothreitol (DTT) assay; acid ascorbic (AA) assay, concentration weighted trajectories (CWT)

Introduction

Exposure to particulate matter (PM) is a major public health issue for all countries in the world. Air quality modelling has revealed that 91% of the global population lives in areas where annual average concentration of $PM_{2.5}$ (particulate matter with an equivalent aerodynamic diameter less than 2.5 µm) exceeds the corresponding WHO guideline limits (10 $\mu g \cdot m^{-3}$) (WHO, 2018). Exposure to the outdoor fine particles has been identified as an important risk factor of mortality with more than 4.2 million premature deaths in the World in 2016 (WHO, 2018). Burnett et al. (2018) applied a new global exposure mortality model to study the association between $PM_{2.5}$ concentration and non-accidental mortality considering 41 cohorts in 16 countries and estimated 8.9 million of $PM_{2.5}$ related deaths in 2015 (Burnett et al., 2018). It is consistent with the 8.8 million recently modelled by Lelieveld et al. (2020). A similar approach applied to the 250 most populates cities in the world predicted a median rate of $PM_{2.5}$-related mortality reaching 39 per 100,000 people, with differences in the cities (13 to 125 deaths per 100,000 people) (Anenberg et al., 2019).

It is well established that particulate matter causes several diseases as lung cancers (Raaschou-Nielsen et al., 2013; Sax et al., 2013), cardiovascular diseases (Massamba et al., 2014), chronic obstructive pulmonary disease (COPD) (Li et al., 2016) and asthma (Bontinck et al., 2020; Hendryx et al., 2019). Toxicological studies have shown that PM has the ability to induce oxidative stress. This latter corresponds to an imbalance between the antioxidant defence and the overproduction of reactive oxygen species (ROS) triggered by an exposure to airborne PM. Oxidative stress appears as an early pathways potentially preceding severe damages to cell components (lipids, proteins and DNA) (Borm et al., 2007; Nel, 2005). The PM composition is a determinant of their ability to contribute to overproduce ROS, and both organic compounds and some metals appeared to be associated with ROS production (Kelly and Fussell, 2012).

Components that contribute mostly to PM mass were found to contribute the least to the toxicity (Borm et al., 2007). For this reason, the PM atmospheric concentration is not the only parameter to consider for assessing the impact of air pollution on human health. Indeed, water soluble major ions as ammonium sulfate, ammonium nitrate and sea-salts are relatively not correlated to the PM toxicity whereas trace elements as Pb, Cd, Ni, As and polycyclic aromatic hydrocarbons as benzo[a]pyrene are known for their high toxicity (Lippmann, 2014) and correspond to regulated species in Europe.

The assessment of toxicological effects of PM related to the oxidative stress is widely investigated considering *in vitro* lung cell exposure (Badran et al., 2020; Gualtieri et al., 2017; Jia et al., 2017). In parallel, acellular tests have been suggested over the last fifteen years to evaluate the PM oxidative potential (OP), which is a measure of the ability of PM to deplete certain antioxidant molecules in synthetic airway fluids (Ayres et al., 2008; Sauvain et al., 2013). The dithiothreitol (DTT) simulates reductant species in cells like Nicotinamide adenine dinucleotide or nicotinamide adenine dinucleotide phosphate. The DTT assay evaluates the ability of PM redox active species to transfer electrons to dissolved molecular oxygen (Kumagai et al., 2002; Li et al., 2003). In the absence of PM redox active species, DTT can act as a reducer of dissolved oxygen leading to formation of H_2O_2. PM components can act as catalyst to increase the reduction of oxygen species to ROS like superoxide anion and H_2O_2. The latter contribute to the overall level of ROS that could be responsible for an oxidative stress in cells. The ascorbic acid (AA) simulates antioxidants in the respiratory tract lining fluid (RTLF) and the AA assay measures the ability of PM to deplete antioxidants in the RTLF (Mudway et al., 2004). The application of DTT and AA assays in many studies showed that they were correlated to both common and different PM constituents. The OP assessed using DTT (OP-DTT) has been correlated not only with metals but also with oxygenated organic compounds (Charrier and Anastasio, 2012; Cho et al., 2005; Crobeddu et al., 2017;

87 Verma et al., 2015). The OP derived from AA assay (OP-AA) has been found correlated
88 rather to metals (Fang et al., 2016; Pietrogrande et al., 2018). An OP assessment based on the
89 use of several assays, as AA and DTT in the present study, appears as an appropriate
90 approach for considering contributions of reactive species from several families of PM
91 components. Information on the relationship between PM components and OP values are
92 sometimes limited since the correlation is based on elements that are specific of a source but
93 not always responsible for the OP response (Gao et al., 2020a). In addition, numerous
94 elements and compounds are emitted by different sources and are not always considered at the
95 analysis step. Therefore, several authors have suggested the investigation of PM source
96 contribution to OP (Calas et al., 2019; Cesari et al., 2019; Yu et al., 2019) as a relevant
97 indicator to identify the sources with high potential toxic effects on human health.
98 In this context, the objective of this study was to relate OP data to PM composition and PM
99 source contribution in an industrial and urban area located in Northern France. The OP-DTT
100 and OP-AA assays were used and relationships between OP results, $PM_{2.5}$ composition and
101 emission sources contributions were investigated by methods including correlation, principal
102 component analysis, bivariate polar plots, concentration roses and concentration weighted
103 trajectories.
104
105 1. Materials and methods
106 1.1. $PM_{2.5}$ samples
107 1.1.1. Study area and sampling.
108 $PM_{2.5}$ samples considered in this work were collected in Dunkerque (latitude:
109 51°2′10″N; longitude: 2°22′46″E) in winter and spring 2010-2011. Since 2010-2011, the
110 $PM_{2.5}$ samples have been stored at -18°C in the dark, in hermetically sealed boxes. This
111 procedure ensures to present any volatilization or transformation of the organic compounds

over time. The detailed description of the sampling methodology and the study area is given in Kfoury et al. (2016). Briefly, Dunkerque, 210,000 inhabitants with its suburbs, is an industrialized city located in Northern France in the southern coast of the North-Sea. Due to its location, this site is significantly influenced by common sources as sea spray, marine traffic, domestic and road traffic emissions as well as more specific sources, notably industrial emissions in the field of metallurgy, cement production and organic chemistry. Between the industrial sources, an integrated steelworks (ISW) which is the biggest steel producer in Europe, and an electric steel plant (ESP) are noticeable and located in the 260–290° wind sector and east to the sampling site respectively (Figure S1). According to the European pollutant release and transfer register (E-PRTR), cumulatively in 2010, all the industries located in Dunkerque region emitted in the air 3,100 tons of total suspended particles including 8,117 kg of Zn, 6,962 kg of Pb, 1,398 kg of Ni, 1,241 kg of Cu, 1,194 kg of Cr, 175 kg of Cd and 101 kg of As (E-PRTR, 2011). $PM_{2.5}$ was collected on a semi-daily basis (00:00–12:00 UTC and 12:00–24:00 UTC time period) using the high volume (30 $m^3 \cdot h^{-1}$) DA80 sampler (DA80, DIGITEL®, Switzerland). Two types of 150 mm diameter filters were used: cellulose (grade 41, Whatman®, GE Healthcare Life Sciences, United Kingdom) for major and trace elements analysis and OP determination, and high purity quartz microfiber filters (grade QM-A, Whatman®, GE Healthcare Life Sciences, United Kingdom) for carbon quantification.

1.2. $PM_{2.5}$ composition and source contribution

$PM_{2.5}$ samples were analyzed for their content in major and trace species as Ag, Al, As, Ba, Bi, Ca, Cd, Co, Cr, Cu, Fe, K, Mg, Mn, Na, Ni, Pb, Rb, Sb, Sn, Sr, Ti, V, Zn, NH_4^+, Cl^-, NO_3^-, SO_4^{2-} and total carbon (TC) using Inductively Coupled Plasma-Mass spectrometry (ICP-MS), Inductively Coupled Plasma Atomic Emission spectroscopy (ICP-AES), ion

chromatography and a CHNS/O elemental analyzer. The detailed protocols are described in Kfoury et al. (2016) and Ledoux et al. (2017).

In a previous study, constrained weighted-non-negative matrix factorization (CW-NMF) was applied to the whole $PM_{2.5}$ composition dataset (173 $PM_{2.5}$ samples) and led to the identification of 11 contributing sources (Kfoury et al., 2016). The eight first ones can be considered as sources typically encountered at an urban coastal site: sea salts, aged sea salts, crustal, heavy fuel oil combustion, combustion 2 (mix between biomass and road traffic combustion) and traffic non-exhaust (related to wear of the car mobile parts such as brakes, tires, clutch …) for which both a local and distant origin can be considered, and secondary sulfates and secondary nitrates which are typically related to long range transport. Three other source profiles were related to the local steelmaking activities located close to the sampling site (less than 7 km): one for the ESP emissions and two for the ISW sources with a distinction for the latter between the sintering stack (ISW-Sintering Stack) and the fugitive emissions from the whole ISW site (ISW-Fugitive).

In this work, 57 out of the 173 $PM_{2.5}$ samples were considered for studying their oxidative potential. The sample selection was made based on $PM_{2.5}$ concentrations and source contributions. $PM_{2.5}$ samples showing higher relative contribution for each of the eleven sources were included in addition to the high (> 50 $\mu g \cdot m^{-3}$) and low (<10 $\mu g \cdot m^{-3}$) $PM_{2.5}$ concentration samples.

1.3. Oxidative potential measurements

OP was assessed by using two a-cellular methods based on the depletion rate of DTT (OP-DTT) and AA (OP-AA) in the presence of the PM constituent. When performing these tests, an important issue is first related to the choice of the leaching agent that will be used for the PM extraction. The latter has to be representative of the physiological conditions

occurring in the PM target organs (Calas et al., 2017; Pietrogrande et al., 2019). As well, the extraction procedure has also an important influence on the OP results and the review of the literature showed large differences between the methods used (Bates et al., 2019). The fact there is no standardized method for OP measurements leads to consider a compromise between all the critical parameters such as solvent, extraction procedure and solid/liquid (S/L) ratio (Hernandez-Pellon et al., 2018).

1.3.1. Sample preparation for OP tests

The Gamble's solution (pH=7.4) is one of the most used simulated lung fluids (SLF) and represents the interstitial fluid in the deep lung. Therefore, it was chosen as a leaching agent for the $PM_{2.5}$ extraction. The Gamble's solution was daily freshly prepared according to the specifications given in Colombo et al. (2008), using ultrapure water and mixing the stock solutions following the order given in Table S1 (see supplementary materials) to avoid salt precipitation. The citrate was used to simulate proteins that can be found in the lung lining fluid and acetate instead of organic acids (Hedberg et al., 2010; Marques et al., 2011). All chemicals were of analytical grades. The pH of the Gamble's solution was adjusted to 7.4 by adding drop-wise HCl 10% (Wragg and Klinck, 2007) or NaOH 1M (Caboche et al., 2011).

For each of the 57 $PM_{2.5}$ samples, about 1/10 of the cellulose filter, containing an average of 1.40 mg of $PM_{2.5}$, was placed in a 15 mL glass tube with 14 mL of Gamble's solution. The volume was chosen in accordance with real human exposure conditions with respect to the ambient concentration of particles, the inhaled air volume and the pulmonary fluid volume. In these conditions, the S/L ratio was in the 1/500 - 1/50000 range avoiding any risk of saturation and competition between the soluble compounds (Caboche et al., 2011).

The extraction tubes were covered with aluminum foil and placed in a heated orbital shaker for 24 h at 37°C, at a speed of 250 oscillations·min^{-1}. Solutions were then filtered on 0.45 µm

187 nylon filters, and the filtrates were placed in flasks, and stored at -20°C until OP analyses.
188 Blanks were considered by treating several field blank filters with the same protocol as
189 applied on $PM_{2.5}$ filters.
190
191 1.3.2. Dithiothreitol OP test
192 Redox-active species in PM have the ability to oxidize DTT to DTT disulfide, and
193 catalyze the reduction of oxygen species to ROS like superoxide anion and H_2O_2. When
194 5,5-dithio-bis-(2-nitrobenzoic acid) (DNTB) is added, the remaining DTT reacts with DTNB,
195 generating DTT-disulfide and 2-nitro-5-thiobenzoic acid (TNB) (Figure S2). The latter is
196 quantified, by measuring its absorbance at 412 nm, which is also proportional to the
197 remaining quantity of DTT (Visentin et al., 2016).
198 The DTT protocol was optimized in a microplate version which makes easier the
199 consideration of several points (i.e. 7 points in this work) for evaluation of the DTT depletion.
200 DTT and DNTB stock solutions were prepared at a concentration of 0.4 mM and 1.5 mM,
201 respectively, in a phosphate buffer (pH=7.4). Since both solutions are sensitive to light and
202 temperature (Damodaran, 1985; Eyer et al., 2003), they were kept in amber glass vials in the
203 dark at -20°C until use. The OP-DTT measurement was carried out in 96 well black plates
204 with clear flat bottom (Coastar® 3631, Corning Incorporated Life Sciences, USA). 120 µL of
205 potassium phosphate buffer (pH=7.4), and 40 µL of the PM leachate (or blank or positive
206 control) were added in each well. The plate was then placed at 37°C for 10 min under
207 shaking. 25 µL of DTT (0.4 mM) was then added to initiate the oxidation reaction.
208 The remaining DTT concentration was estimated after 0, 5, 10, 20, 30, 45 and 60
209 minutes of reaction between PM leachate components and DTT, at 37°C. After each time of
210 reaction, 15 µL DTNB were then added to each well to convert remaining DTT to TNB. After
211 10 min at 37°C, the absorbance of TNB was measured at 412 nm (spectrophotometer

Multiskan Go, Thermo Fisher Scientific, Finland), and converted to DTT remaining quantity. The DTT depletion rate was calculated using the slope of the curve (linear regression) of remaining DTT versus time. 1.4 naphthoquinone (1.4 NQ), 100 µM, was used as a positive control and obtained values (1.23 $\mu M \cdot min^{-1}$) were in the range of those obtained in the literature.

For each $PM_{2.5}$ sample, OP-DTT values were obtained by correcting the $PM_{2.5}$ filter slope values with the blank filter one. Samples were analyzed in triplicates and the given OP-DTT values correspond to the arithmetic mean. The relative standard deviation was below 4.1 %. The OP-DTT values were finally expressed per unit of mass of PM (OP-DTTm in $pmol \cdot min^{-1} \cdot \mu g^{-1}$) and per unit of air volume (OP-DTTv in $nmol \cdot min^{-1} \cdot m^{-3}$). The first unit can be related to the intrinsic OP of 1 µg of emitted PM and will be used to compare OP of the sources. The second one can be related to the intrinsic OP of 1 m^3 of the air people breathe and is more adapted for studying the situation (wind direction and air mass origin…) in which the impact on health could be high.

1.3.3. Ascorbic acid OP test

AA is present in the lung epithelial lining fluid (ELF), along with other antioxidants like reduced glutathione (GSH), and uric acid (UA). Since AA has the same response, weather in a mixture of these antioxidants or alone, it can be used as a simplified model of the synthetic respiratory tract lining fluid (Zielinski et al., 1999). As for DTT, the redox active species in PM have the ability to oxidize AA to dehydroascorbic acid (Figure S2), and catalyze the formation of ROS by transferring an electron to oxygen molecules. AA stock solution (1 mM) was prepared in ultrapure water, and stored at -20°C due to its instability at room temperature (Bode et al., 1990). The OP-AA measurement was done in 96 well plates with UV-transparent flat bottom (UV-Star® 655801, Greiner bio-one, Austria). 160 µL of PM

leachate was placed in each well of the plate, and the latter was heated to 37°C (5 min), before adding 40 µL of AA solution and shaking for 1 min. Finally, the plate was placed in the spectrophotometer (Multiskan Go, Thermo Fisher Scientific, Finland), at 37°C and the absorbance was measured at 265 nm every 2 minutes for 2 h (Jung and Wells, 1998) with a 30 s shaking step before each measurement (Yang et al., 2014). OP-AA values were deduced from the AA depletion curve versus time considering the slope of the linear part of the curve, where AA depletion rate is maximal. Samples were analyzed in triplicates (RSD < 3.7 %), blank filters were considered, 1.4 NQ was used as positive control (2.74 $\mu M \cdot min^{-1}$) and OP-AA values were expressed per unit of mass of PM and volume (OP-AAm and OP-AAv respectively).

1.4. Data handling and processing

Relationships between OP results, $PM_{2.5}$ composition and source contributions were investigated by using several methods including correlation, principal component analysis (PCA), bivariate polar plots, concentration roses, OP roses and concentration weighted trajectories (CWT). The R software was used in addition to FactomineR (Lê et al., 2008) and openair (Carslaw and Ropkins, 2012) packages to perform these calculations.

1.4.1. Correlation

Prior the determination of the correlation coefficient between the variables under study, the Shapiro-Wilk test was performed to assess the normality of the data distribution. As the normality was not verified ($p < 0.001$) for most of the variables, the Spearman correlation coefficient was used. Two levels of significance were considered, $p < 0.05$ and $p < 0.001$,

allowing to conclude about the correlation with 95% and 99.9% of confidence respectively. In addition, correlations were also investigated by using PCA after data normalization.

1.4.2. Bivariate polar plots and concentrations roses.

Bivariate polar plots and OP and concentration roses were used to investigate the relationships between OP values and contribution of local sources.

Bivariate polar plots represent the variation of a quantitative parameter (concentration, OP value, source contribution) versus the wind direction and wind speed. For each $PM_{2.5}$ sample, the parameter values obtained for the 12 h period were distributed in front of the 12 corresponding hourly wind speed and directions. The data set used to draw each polar plot counts 57x12 lines. The OP and concentration roses, which give the average value in a particular wind direction, were calculated using the same dataset after averaging the values at 45° intervals.

1.4.3. Concentration weighted trajectories

The concentration weighted trajectories (CWT) (Cheng et al., 2013; Dimitriou et al., 2015) were used to investigate relationships between OP and distant sources. The CWT methods assume that when an air mass is passing through a polluted area, the material can be transported along the trajectory to the receptor site. By using air mass back-trajectories and affecting values observed at the receptor site along the trajectories, it is possible, by the end after averaging, to locate areas responsible for high values (Carslaw, 2019).

Air mass back-trajectories were calculated using the hybrid single particles Lagrangian integrated trajectory (HYSPLIT) model (Rolph et al., 2017; Stein et al., 2015) considering the Gridded Meteorological Data Archives (GDAS 0.5 degrees) and a height of 100 meters above ground level at receptor site. For each $PM_{2.5}$ sample, four 72 h backward trajectories were

assigned (one trajectory every 3 hours) and OP and source contribution values obtained for the 12 hours period were merged with the 4 corresponding trajectories. The dataset used for CWT calculation count 72x4x57 lines.

2. Results and discussion

2.1. $PM_{2.5}$ composition et sources contribution

Table 1 regroups the average composition of the $PM_{2.5}$ samples and Table 2 summarizes the chemical markers that were used for identifying the sources as well as their average contributions (Kfoury et al., 2016). The $PM_{2.5}$ average concentration of the selected samples was 29.2 $\mu g \cdot m^{-3}$, which is similar to the average concentration typically encountered during the winter-spring period in the studied area (Kfoury et al., 2016). Among the PM components, NO_3^-, TC, SO_4^{2-}, NH_4^+, Cl^-, and Na showed the highest average concentrations (> 300 $ng \cdot m^{-3}$) representing together about 67% of the $PM_{2.5}$ mass. These elements appeared characteristics of the secondary nitrate and sulfate source profiles as well as the combustion and the marine sources (Table 2). NH_4^+ and Cl^- are also characteristic elements of the ISW sintering stack emissions (Hleis et al., 2013). Fe, K, Ca, Mg and Al were found with concentrations between 26 and 155 $ng \cdot m^{-3}$. These elements are known to belong to the aluminosilicates category. Nevertheless, at Dunkerque urban-industrial site, they were shown to be also associated with emissions from the ISW (Hleis et al., 2013) and notably dusts from the sintering unit. Among the trace metals, Zn (67.6 $ng \cdot m^{-3}$), Pb (14.8 $ng \cdot m^{-3}$) and Mn (13.7 $ng \cdot m^{-3}$) stand out and were mainly associated with the metallurgical activities occurring in the ESP and the ISW (Table 2).

2.2. OP-AA and OP-DTT average values

310 The average mass- and volume-normalized OP-DTT and OP-AA values at Dunkerque
311 site are presented together with values published for other European and world sites in
312 Table 3, together with the leaching agents used for extracting PM samples. Ultrapure water,
313 ethanol, methanol, water, phosphate buffer and Gamble solution were used for leaching in
314 addition to ultrasonic treatment or shaking for various times. In one study only , the solution
315 was not filtered after extraction (Janssen et al., 2014). The heterogeneity of the methodologies
316 used could influence the obtained values and could make the comparison not reliable. As the
317 leaching agent is different, the response could also be different as published by Calas et al.
318 (2017) who compared responses in OP_DTT test on extracts obtained by using artificial
319 lysosomal fluid (ALF), ultrapure water, Gamble solution and Gamble solution implemented
320 with dipalmitoylphosphatidylcholine. Based on the analysis of 5 different PM samples,
321 including four real PM samples, it was shown that OP values observed using the ultrapure
322 water were always slightly higher than those obtained using the Gamble solution.
323 Nevertheless, focusing on the real PM samples, the difference was not exceeding 13% which
324 make reliable the comparison between values obtained using ultrapure water and Gamble
325 solution. In most of the comparison studies included in table 3, ultrapure water was used as
326 leaching agent. Solubility is also highly dependent of the pH of the leaching agent
327 (Hernandez-Pellon et al., 2018). As the phosphate buffer has the same pH value as the
328 Gamble solution (7.4), we can assume that OP values could be compared without severe bias.
329 However, Jedynska et al. (2017) used methanol as leaching agent and the leachate probably
330 concentrates more organic constituents than leachates obtained using Gamble, water or
331 phosphate buffer. In contrast to the other studies, Janssen et al. (2014) did not filter extracts
332 before testing OP which leads to the inclusion of the contributions of insoluble species in OP
333 values. Consequently, except for Jedynska et al. (2017), who used methanol and Janssen et al.

(2014), we can be confident with the reliability of the comparison between values from the cited papers.

Focusing on values related to $PM_{2.5}$ concentration, the average ± standard deviation OP-DTTv value, 0.36 ± 0.24 $nmol \cdot min^{-1} \cdot m^{-3}$, appeared in accordance with values observed in urban and urban background sites such as Paris (France), Atlanta (USA), Lecce (Italy), Athens (Greece) (Chirizzi et al., 2017; Gao et al., 2020b; Jedynska et al., 2017; Paraskevopoulou et al., 2019). On the other hand, OP-DTTv value is lower than the one determined in Beijing and Hangzhou (China) or in Patalia (India) (Patel and Rastogi, 2018; Wang et al., 2019; Yu et al., 2019). Except for the Netherlands, the corresponding $PM_{2.5}$ concentrations are also far higher (> 113 $\mu g \cdot m^{-3}$) than Dunkerque one. The average OP-DTTm, 17.7 ± 15.4 $pmol \cdot min^{-1} \cdot \mu g^{-1}$, OP-AAv, 1.12 ± 1.15 $nmol \cdot min^{-1} \cdot m^{-3}$ and OP-AAm values, 55 ± 66 $pmol \cdot min^{-1} \cdot \mu g^{-1}$ were also comparable to the range published for European, Asian and American sites.

2.3. Correlation of OP with chemical species and source contributions

In order to study the contribution of PM chemical components to the DTT and AA oxidation activity, the correlation between OP-DTTv and OP-AAv values and the chemical species was investigated based on the Spearman correlation coefficients (Table 4) and PCA (Figure 1 and Table S2).

2.3.1. Spearman correlation

OP-DTTv and OP-AAv showed statistically significant correlation ($p < 0.05$) with almost all the species under study (Table 4). However, they were not correlated with Ca and Cl^-, while Al, Co, V were only correlated with OP-DTTv, and Sr only with OP-AAv. Stronger correlations were globally observed between the PM components and OP-DTTv compared to

OP-AAv. This latter observation is consistent with results from other research groups (Calas et al., 2019; Fang et al., 2016). In particular, Ag, Al, As, Ba, Bi, Cd, Co, Cr, Cu, Fe, K, Mn, Ni, Pb, Rb, Sb, Sn, Zn, NO_3^- and TC showed correlation coefficient higher than 0.6 with OP-DTTv. Such a correlation level was observed only for As, Ba, Cu, Na, Pb, Sb, Sn and TC with OP-AAv. A very strong correlation was found between OP-DTTv and Cu ($r = 0.85$), Cd ($r = 0.82$) and Sn ($r = 0.82$).

The major PM components TC, SO_4^{2-} NO_3^- and NH_4^+ appeared more correlated with OP-DTTv than OP-AAv. This is consistent with the stronger correlation found between $PM_{2.5}$ concentrations and OP-DTTv in comparison with OP-AAv ($r = 0.67$ versus $r = 0.45$ respectively). Our results are in agreement with other observations showing that secondary inorganic aerosols (SIA) components were correlated with OP-DTT (Ma et al., 2018; Paraskevopoulou et al., 2019; Wang et al., 2019). On the contrary, Mg, Na and Sr showed negative correlation coefficients with OP values. These elements are mainly related to the marine influence at the study site. Finally a moderate correlation ($r = 0.46$, $p < 0.001$) was found between OP-DTTv and OP-AAv which indicates that the two tests do not exactly respond to the same species and prove the complementarity between both.

AA and DTT tests respond to the oxidative species solubilized in the gamble solution after leaching of the collected PM. The leachate includes not only the PM components that were identified and quantified, but also unanalyzed PM species. These latter, such as water soluble organic carbon (WSOC) including humic-like substances (HULIS) or oxygenated PAH, are an integral part of the leachate and also contribute to the OP values as well (Bates et al., 2019; Gao et al., 2020a; Jiang et al., 2020; Lin and Yu, 2019; Ma et al., 2018). In this study, the inorganic PM composition has been investigated and, based on this, the CW-NMF model allowed to determine the source contributions. Consequently, studying the correlation

between OP values and source contributions allows indirectly to consider all the species including the WSOC related to a specific source whether they have been analyzed or not.

Strong correlations ($r \geq 0.6$) were found between the "traffic non-exhaust", "secondary nitrates", "ISW fugitive", "ISW sintering stack" and "electric steel plant" sources contribution and OP-DTT values. The three industrial sources are known to emit metals with redox properties (E-PRTR, 2011; Hleis et al., 2013; Kfoury et al., 2016) able to potentiate ROS overproduction. “Secondary sulfates” and "heavy fuel oil combustion" were moderately correlated ($0.4 \leq r < 0.6$) with only OP-DTTv. Considering the mass normalized data (Table S3 in supplementary materials), OP-DTTm appeared strongly correlated with "ISW fugitive", moderately correlated with "traffic non exhaust", "heavy fuel oil combustion", "crustal" and "ISW sintering stack" while no correlation was found with secondary nitrates and only poor correlation with secondary sulfates ($r=0.35$). Except for "aged sea-salts" ($r = -0.67$) and "traffic non-exhaust" ($r = 0.66$), OP-AAv only showed, at best, moderate correlations with the contribution of each of the 11 sources. Interestingly "sea-salts" and "aged sea-salts" sources show negative correlations with OP-DTTv and OP-AAv values. However, it would be wrong to conclude that emissions related to these sources are able to decrease the OP values. Indeed, in the urban coastal area under study, high marine contributions are associated with high speed winds and favorable condition of dispersion (Ledoux et al., 2006). Consequently, when the marine origin is predominant, the $PM_{2.5}$ concentration tends to be relatively low (Figure S3 and Figure S4) and metal concentration values as well, which could explain the low OP values. Finally, no significant correlation was found with the "crustal" source suggesting that this latter does not significantly contribute to the OP values.

2.3.2. Principal Component Analysis

Unlike Spearman correlation which tests the correlation between pairs of variables, the PCA is a multivariate analysis. It also allows to evidence discrete relationships between variables that will be regrouped as components. PCA was applied to the composition data of the 57 $PM_{2.5}$ samples for the 29 studied species concentration. The source contributions and OP values were considered as supplementary variables.

The 5 first obtained axes explain 71.7% of the data variability. As OP-AAv and OP-DTTv showed only significant correlation coefficients with the two first principal components, the focus was only done on these latter (Figure 1 and Table S2). The variable factor map of the two major axes which represent together 47.1% of the total variance is presented in Figure 1c. Axis 1 is highly positively associated with metals (from high to low r value with $r > 0.6$: Bi, K, Rb, Ag, Sn, As, Fe, Al, Ti, Pb, Mn, Ba, Co, TC and Ni) and negatively associated with Na. So the first axis evidenced that several metals are correlated and that when a concentration is high for one these elements, all the concentrations tends to be also high for the others. From lower to higher values, axis 1 makes the distinction between the typical sea components and the typical metals emitted by anthropogenic and industrial activities. NH_4^+, NO_3^-, SO_4^{2-} and TC are negatively correlated with the second axis while Na, Sr, Ca and Mg are positively correlated. Hence, the second axis makes the distinction between the typical sea components (positive part of the axis) and the SIA (negative part of the axis). In the region where the study takes place, SIA are mainly associated with winds blowing from the East (continent) and long range transport while marine aerosol are mainly originates from the North and western direction. When the marine contribution is high, the secondary aerosol contribution tends to be low (Figure S3). This explains why SIA are placed against sea-salts components on the second axis. NH_4^+, NO_3^-, SO_4^{2-} and TC contribute the most to the $PM_{2.5}$ mass, and a strong correlation ($r = -0.70$) was found between the $PM_{2.5}$ concentration and the second axis.

OP-DTTv was very strongly correlated (r = 0.84) with the first axis as a consequence of the clear relationships between DTT test values and metal concentrations while OP-AAv appeared only moderately anticorrelated (r = -0.48) with the second axis. Considering now both dimensions but only 47.1% of the data variability, OP-AAv was related to the "secondary nitrates", "secondary sulfates" and "combustion 2" (road traffic and biomass combustion) sources. OP-AAv was also very strongly anticorrelated with "sea-salts" and "aged sea-salts" sources. This result was not so well evidenced considering the whole data variability by studying the correlation coefficient. Then for OP-DTTv, PCA findings were mixed as it was only correlated with axis 1. Considering axes 1 and 2, only one clear relationship appeared with the ISW sintering stack while several ones were evidenced from the correlation coefficient study. A deepest investigation will be done hereafter.

2.4. OP values and relationship with local and distant sources

Concentration roses and bivariate polar plots were used to study the link between OP observed values and local sources contribution while CWT was used to search for regional influences.

2.4.1. Mass-normalized and volume-normalized OP

Roses representing OP value versus wind direction and bivariate polar plots considering OP expressed in the two units (per m^3 or per µg $PM_{2.5}$) are given in Figure 2. OP-AA and OP-DTT did not exhibit exactly the same behavior regarding the wind direction. The maximum for mass-normalized OP-AAm and OP-DTTm was obtained when the wind blew from the northwest (NW) wind sector, while the maximum for volume-normalized OP was related to the southeast (SE) wind direction for OP-AAm, and SE, west (W) and northeast (NE) direction for OP-DTTm. The W-NW and the SE sectors correspond to the

industrial park including the ISW and the urban sector, respectively, while in the northeast direction is located the electric steel plant.

Especially when considering the OP-AA values, 1 µg of PM coming from the wind sector including the industrial park showed the maximum intrinsic oxidative potential compared to an equivalent mass of PM sampled from the others wind sectors. By normalizing OP values to the air volume, this sector no longer exhibited the highest value. This is important information derived from this study. Considering 1 m^3 of air that people breathe, emissions from the industrial park do not appear as the most impacting on OP values. At our study site, emissions from the SE sector corresponding locally to the urban sector or long range transport influence (as it will be seen in section 2.4.3) appear to be the most problematic, considering OP-AAv values. However, the OP-DTTv values showed not only a maximum under the urban sector but also when the winds blew from the west direction suggesting a high OP-DTTv potential for a source located in the industrial park.

2.4.2. OP relationships with the 11 identified CW-NMF sources

Figure 3 represents the volume-normalized source contributions bivariate polar plots of the 11 identified $PM_{2.5}$ emission sources in addition to the one for $PM_{2.5}$ concentrations, for comparison with the corresponding OP-DTTv and OP-AAv one. The use of bivariate polar plots gives an additional strong criterion for validating the relationships between OP values and PM source contribution evidenced with the Spearman correlation and PCA mathematical tools. By using this, OP and source contribution values are distributed versus the wind direction and wind speed. The geographical position of the sources as well the characteristics of the emission (ie: resuspension or blowing back of chimney emission to ground level under the effect of wind speed) are directly and indirectly considered when bivariate polar plots are investigated (Carslaw et al., 2006; Ledoux et al., 2018). It makes possible to deepen

investigation and strengthen conclusions regarding relationships between OP values and source contributions.

Clearly OP-AAv showed a pattern similar to that of $PM_{2.5}$ and road traffic and biomass combustion ("combustion 2"). HULIS could be the reason of the relationship between OP and combustion sources as they are highly redox active species known to participate to the OP values and mainly emitted by combustion processes (Dou et al., 2015; Ma et al., 2018).This observation is also consistent with the one of Yu et al. (2019), who found that vehicle emissions (traffic exhaust and non-exhaust as a whole) highly contribute to ROS production. Based on the polar plot patterns, traffic non-exhaust could also participate to OP-AAv but the absence of correlation between both would suggest to reject the idea. These first observations are in agreement with the PCA findings (Figure 1). However, PCA was suggesting a relationship between OP-AAv and the secondary inorganic aerosols for 47.1% of the data. The bivariate polar plots tend to discredit this as the corresponding plots are quite different (Figure 2 and Figure 3). Except with the $PM_{2.5}$, combustion 2 and possibly traffic non-exhaust source, OP-AAv pattern do not show any similarity with other sources, which could be contradictory with partial conclusion done from the correlation coefficient study. This tends to demonstrate that investigations using only the correlation coefficient between sources contribution (or species concentrations) and OP are not enough to conclude about relationships.

Unlike OP-AAv, OP-DTTv bivariate polar plot showed similarities and compatibilities with several sources. Between them, the ISW sintering stack seems to be responsible for the spot observed in the west direction at a wind speed close to 5 $m \cdot s^{-1}$. In the same direction, the ISW fugitive and the heavy-fuel oil combustion source are also possible contributors. In addition, in the east-northeast wind direction, the OP-DTTv concentration spot overlap the one observed for the electric steel plant making emissions relate to this source another

OP-DDTv influencing factor. Relatively high values observed in the SE quarter could be the fact of combustion 2 or traffic non-exhaust sources. In this case, observations matched quite well those done from PCA study but also contradict again some conclusions done using the correlation coefficient. For example strong correlation was found between secondary nitrates and OP-DTTv ($r = 0.67$, $p < 0.001$), but their respective bivariate polar plots could challenge it. Finally, our observation made possible to definitely dismiss the contribution of the sea-salts, aged sea-salts, crustal and secondary sulfates to the OP values.

Up to our knowledge, this is the first time that bivariate polar plots of OP and sources contributions were compared to study and validate the influence of source emission on OP values. In most of the published works, only correlation coefficients are used to conclude on relationships between OP and species /sources. This could be inadequate in light of our results which clearly demonstrate the interest to use bivariate polar plots as additional information.

2.4.3. Regional influence

The computing of OP-AAv and OP-DTTv with the air-mass back trajectories using the CWT method allowed to study the impact of regional emissions on OP values (Figure 4). Regions contributing the most to OP-DTTv are inland, including the upper part of the western continental Europe notably France, Belgium, Germany and Poland. For OP-AAv, the main hotspot is located in Belgium and the center of Germany. Long range transport from these source regions located east to the study site could also explain the high OP values locally observed for eastern and southeastern wind on the bivariate polar plots. The North-Sea, the English Channel and the coastal part of the Atlantic Ocean appears also as source region especially for the OP-DTTv. This is in agreement with the relationships previously found between OP-DTTv and heavy fuel oil combustion source and the CWT obtained for the latter is also consistent with this. To be mentioned here that the English Channel and the North Sea

532 are among the most used shipping routes for marine transportation (EEA, 2013b; Ledoux et
533 al., 2018).
534 CWT results for secondary nitrates evidenced mainly Belgium and southern part of
535 Netherlands as source regions which is consistent with Pay et al. (2010) and Pay et al. (2012)
536 who identify these countries as important NO_x emitters. Secondary sulfates were originated
537 from Belgium, North of Germany and Poland who also showed exceedances of the SO_2 limit
538 value (EEA, 2012). In both cases, the similarity with the OP-AA_V and OP-DTTv CWT is
539 poor.
540 The highest concentrations of $PM_{2.5}$ were traced back to North of France, Belgium,
541 Luxembourg, Netherlands and Germany also. This is consistent with the potential source
542 contribution results obtained by Waked et al. (2018) and Pay et al. (2012) who evidenced
543 these countries as important source of PM_{10} in relation with industrial and shipping related
544 emissions especially for Belgium and Netherlands. Combustion 2 and traffic non-exhaust
545 CWT patterns showed higher concentrations on the continent which is totally in agreement
546 with the definition of the sources. Source regions of biomass and traffic related combustion
547 traffic-non-exhaust emissions match quite well the OP-DTTv and OP-AAv CWT confirming
548 the relationships suggested at a local scale. Eastern Europe, especially Bulgaria, Czech
549 Republic and Poland, was also identified as an important source of PM in Europe (EEA,
550 2013a). Nevertheless, we were unable to observe their influence as there were no air masses
551 coming from these regions during the sampling period.
552
553 Conclusion
554 $PM_{2.5}$ collected in a coastal industrial city in Northern France was responsible for OP
555 values in the same order of magnitude as those encountered in other world locations. $PM_{2.5}$
556 concentrations, some $PM_{2.5}$ components and $PM_{2.5}$ sources were found to be specifically

557 correlated with one of the two tests (AA and DTT). For one of the first time, bivariate polar
558 plots drawn for OP and source contributions were considered together to investigate their
559 relationships. Conclusions deduced from correlation coefficient studies and PCA were
560 challenged after using the OP and source contribution bivariate polar plots suggesting the
561 importance to use such a methodology. Ascorbic acid assay results appeared clearly linked to
562 the $PM_{2.5}$ concentrations and combustion sources. Dithiothreitol assay was clearly related to
563 sources emitting metals, in our case ISW diffuse and sintering stack, electric steel plant
564 emissions, heavy fuel oil combustion and possibly other combustion sources. Sea-salts, aged
565 sea-salts, crustal, secondary sulfates and secondary nitrates sources do not seem to contribute
566 to OP values. Some high OP values source regions have also been identified (Germany,
567 Belgium and Netherlands) showing that long range transport is also a parameter to consider
568 when studying OP of particulate matter.
569
570 Acknowledgments
571 The "Unité de Chimie Environnementale et Interactions sur le Vivant", UCEIV UR4492,
572 participates in the CLIMIBIO project, which is financially supported by the Hauts-de-France
573 Region Council, the Ministry of Higher Education and Research, the European Regional
574 Development Funds. Lamia Moufarrej is grateful to the "Pôle Métropolitain Côte d'Opale"
575 (PMCO) for the funding of her PhD. The authors gratefully acknowledge the NOAA Air
576 Resources Laboratory (ARL) for the provision of the HYSPLIT transport and dispersion
577 model and/or READY website (http://www.ready.noaa.gov) used in this publication.
578
579
580

581 References

582 Anenberg, S.C., Achakulwisut, P., Brauer, M., Moran, D., Apte, J.S., Henze, D.K., 2019.
583 Particulate matter-attributable mortality and relationships with carbon dioxide in 250
584 urban areas worldwide. Sci Rep 9, 11552. (10.1038/s41598-019-48057-9)
585 Ayres, J.G., Borm, P., Cassee, F.R., Castranova, V., Donaldson, K., Ghio, A., Harrison, R.M.,
586 Hider, R., Kelly, F., Kooter, I.M., Marano, F., Maynard, R.L., Mudway, I., Nel, A.,
587 Sioutas, C., Smith, S., Baeza-Squiban, A., Cho, A., Duggan, S., Froines, J., 2008.
588 Evaluating the toxicity of airborne particulate matter and nanoparticles by measuring
589 oxidative stress potential--a workshop report and consensus statement. Inhal. Toxicol.
590 20, 75-99. (10.1080/08958370701665517)
591 Badran, G., Verdin, A., Grare, C., Abbas, I., Achour, D., Ledoux, F., Roumié, M., Cazier, F.,
592 Courcot, D., Lo Guidice, J.-M., Garçon, G., 2020. Toxicological appraisal of the
593 chemical fractions of ambient fine (PM2.5-0.3) and quasi-ultrafine (PM0.3) particles in
594 human bronchial epithelial BEAS-2B cells. Environ. Pollut. 263, 114620.
595 (10.1016/j.envpol.2020.114620)
596 Bates, J.T., Fang, T., Verma, V., Zeng, L., Weber, R.J., Tolbert, P.E., Abrams, J.Y., Sarnat,
597 S.E., Klein, M., Mulholland, J.A., Russell, A.G., 2019. Review of Acellular Assays of
598 Ambient Particulate Matter Oxidative Potential: Methods and Relationships with
599 Composition, Sources, and Health Effects. Environ. Sci. Technol. 53, 4003-4019.
600 (10.1021/acs.est.8b03430)
601 Bode, A.M., Cunningham, L., Rose, R.C., 1990. Spontaneous decay of oxidized ascorbic acid
602 (dehydro-L-ascorbic acid) evaluated by high-pressure liquid chromatography. Clin.
603 Chem. 36, 1807-1809.
604 Bontinck, A., Maes, T., Joos, G., 2020. Asthma and air pollution: recent insights in
605 pathogenesis and clinical implications. Curr. Opin. Pulm. Med. 26, 10-19.
606 (10.1097/mcp.0000000000000644)
607 Borm, P.J.A., Kelly, F., Künzli, N., Schins, R.P.F., Donaldson, K., 2007. Oxidant generation
608 by particulate matter: from biologically effective dose to a promising, novel metric.
609 Occup. Environ. Med. 64, 73-74. (10.1136/oem.2006.029090)
610 Burnett, R., Chen, H., Szyszkowicz, M., Fann, N., Hubbell, B., Pope, C.A., Apte, J.S., Brauer,
611 M., Cohen, A., Weichenthal, S., Coggins, J., Di, Q., Brunekreef, B., Frostad, J., Lim,
612 S.S., Kan, H., Walker, K.D., Thurston, G.D., Hayes, R.B., Lim, C.C., Turner, M.C.,
613 Jerrett, M., Krewski, D., Gapstur, S.M., Diver, W.R., Ostro, B., Goldberg, D., Crouse,
614 D.L., Martin, R.V., Peters, P., Pinault, L., Tjepkema, M., van Donkelaar, A.,
615 Villeneuve, P.J., Miller, A.B., Yin, P., Zhou, M., Wang, L., Janssen, N.A.H., Marra, M.,
616 Atkinson, R.W., Tsang, H., Quoc Thach, T., Cannon, J.B., Allen, R.T., Hart, J.E.,
617 Laden, F., Cesaroni, G., Forastiere, F., Weinmayr, G., Jaensch, A., Nagel, G., Concin,
618 H., Spadaro, J.V., 2018. Global estimates of mortality associated with long-term
619 exposure to outdoor fine particulate matter. Proceedings of the National Academy of
620 Sciences 115, 9592. (10.1073/pnas.1803222115)
621 Caboche, J., Esperanza, P., Bruno, M., Alleman, L.Y., 2011. Development of an in vitro
622 method to estimate lung bioaccessibility of metals from atmospheric particles. Journal
623 of environmental monitoring: JEM 13, 621-630. (10.1039/c0em00439a)
624 Calas, A., Uzu, G., Besombes, J.L., Martins, J.M.F., Redaelli, M., Weber, S., Charron, A.,
625 Albinet, A., Chevrier, F., Brulfert, G., Mesbah, B., Favez, O., Jaffrezo, J.L., 2019.
626 Seasonal variations and chemical predictors of oxidative potential (OP) of particulate
627 matter (PM), for seven urban French sites. Atmosphere 10. (10.3390/atmos10110698)
628 Calas, A., Uzu, G., Martins, J.M.F., Voisin, D., Spadini, L., Lacroix, T., Jaffrezo, J.L., 2017.
629 The importance of simulated lung fluid (SLF) extractions for a more relevant evaluation

of the oxidative potential of particulate matter. Sci. Rep. 7, 11617. (10.1038/s41598-017-11979-3)
Carslaw, D., 2019. The openair manual - open-source tools for analysing air pollution data. Manual for version 2.6-6, University of York, p. 229.
Carslaw, D., Ropkins, K., 2012. openair - An R package for air quality data analysis. Environ. Modell. Softw. 27-28, 52-61. (10.1016/j.envsoft.2011.09.008)
Carslaw, D.C., Beevers, S.D., Ropkins, K., Bell, M.C., 2006. Detecting and quantifying aircraft and other on-airport contributions to ambient nitrogen oxides in the vicinity of a large international airport. Atmos. Environ. 40, 5424-5434. (https://doi.org/10.1016/j.atmosenv.2006.04.062)
Cesari, D., Merico, E., Grasso, F.M., Decesari, S., Belosi, F., Manarini, F., de Nuntiis, P., Rinaldi, M., Volpi, F., Gambaro, A., Morabito, E., Contini, D., 2019. Source apportionment of $PM_{2.5}$ and of its oxidative potential in an industrial suburban site in South Italy. Atmosphere 10. (10.3390/ATMOS10120758)
Charrier, J.G., Anastasio, C., 2012. On dithiothreitol (DTT) as a measure of oxidative potential for ambient particles: evidence for the importance of soluble transition metals. Atmos. Chem. Phys. 12, 11317-11350. (10.5194/acpd-12-11317-2012)
Cheng, I., Zhang, L., Blanchard, P., Dalziel, J., Tordon, R., 2013. Concentration-weighted trajectory approach to identifying potential sources of speciated atmospheric mercury at an urban coastal site in Nova Scotia, Canada. Atmos. Chem. Phys. 13, 6031-6048. (10.5194/acp-13-6031-2013)
Chirizzi, D., Cesari, D., Guascito, M., Dinoi, A., Giotta, L., Donateo, A., Contini, D., 2017. Influence of Saharan dust outbreaks and carbon content on oxidative potential of water-soluble fractions of $PM_{2.5}$ and PM_{10}. Atmos. Environ. 163. (10.1016/j.atmosenv.2017.05.021)
Cho, A.K., Sioutas, C., Miguel, A.H., Kumagai, Y., Schmitz, D.A., Singh, M., Eiguren-Fernandez, A., Froines, J.R., 2005. Redox activity of airborne particulate matter at different sites in the Los Angeles Basin. Environ. Res. 99, 40-47. (10.1016/j.envres.2005.01.003)
Colombo, C., Monhemius, A.J., Plant, J.A., 2008. Platinum, palladium and rhodium release from vehicle exhaust catalysts and road dust exposed to simulated lung fluids. Ecotoxicol. Environ. Saf. 71, 722-730. (10.1016/j.ecoenv.2007.11.011)
Crobeddu, B., Aragao-Santiago, L., Bui, L.-C., Boland, S., Baeza Squiban, A., 2017. Oxidative potential of particulate matter 2.5 as predictive indicator of cellular stress. Environ. Pollut. 230, 125-133. (https://doi.org/10.1016/j.envpol.2017.06.051)
Damodaran, S., 1985. Estimation of disulfide bonds using 2-nitro-5-thiosulfobenzoic acid: limitations. Anal. Biochem. 145, 200-204.
Dimitriou, K., Remoundaki, E., Mantas, E., Kassomenos, P., 2015. Spatial distribution of source areas of $PM_{2.5}$ by Concentration Weighted Trajectory (CWT) model applied in PM2.5 concentration and composition data. Atmos. Environ. 116, 138-145. (https://doi.org/10.1016/j.atmosenv.2015.06.021)
Dou, J., Lin, P., Kuang, B.-Y., Yu, J.Z., 2015. Reactive Oxygen Species Production Mediated by Humic-like Substances in Atmospheric Aerosols: Enhancement Effects by Pyridine, Imidazole, and Their Derivatives. Environ. Sci. Technol. 49, 6457-6465. (10.1021/es5059378)
E-PRTR, 2011. The European Pollutant Release and Transfer Register. European Environment Agency. http://prtr.ec.europa.eu. Assessed June 09, 2020.
EEA, 2012. European Environmental Agency - Air Quality in Europe - Report No 4/2012. Office for Official Publications of the European Union, 2012, Luxembourg, 108 p.

EEA, 2013a. European Environmental Agency - Air Quality in Europe - 2013 Report. Technical Report No 09/2013. EEA, Copenhagen. Publications Office of the European Union, 112 p.

EEA, 2013b. European Environmental Agency. The impact of international shipping on European air quality and climate forcing. Technical report No 4/2013. Publications Office of the European Union, 2013, Luxembourg, 84 p.

Eyer, P., Worek, F., Kiderlen, D., Sinko, G., Stuglin, A., Simeon-Rudolf, V., Reiner, E., 2003. Molar absorption coefficients for the reduced Ellman reagent: reassessment. Anal. Biochem. 312, 224-227.

Fang, T., Verma, V., Bates, J.T., Abrams, J., Klein, M., Strickland, M.J., Sarnat, S.E., Chang, H.H., Mulholland, J.A., Tolbert, P.E., Russell, A.G., Weber, R.J., 2016. Oxidative potential of ambient water-soluble $PM_{2.5}$ in the southeastern United States: contrasts in sources and health associations between ascorbic acid (AA) and dithiothreitol (DTT) assays. Atmos. Chem. Phys. 16, 3865-3879. (https://doi.org/10.5194/acp-16-3865-2016)

Gao, D., Godri Pollitt, K.J., Mulholland, J.A., Russell, A.G., Weber, R.J., 2020a. Characterization and comparison of $PM_{2.5}$ oxidative potential assessed by two acellular assays. Atmos. Chem. Phys. 20, 5197-5210. (10.5194/acp-20-5197-2020)

Gao, D., Mulholland, J.A., Russell, A.G., Weber, R.J., 2020b. Characterization of water-insoluble oxidative potential of PM2.5 using the dithiothreitol assay. Atmos. Environ. 224. (10.1016/j.atmosenv.2020.117327)

Gualtieri, M., Ledoux, F., Verdin, A., Billet, S., Martin, P.J., Courcot, D., 2017. Particulate matter physico-chemical characterization and *in vitro* toxicological effects, Chapter 12, in: Kumar, D.P. (Ed.), Airborne Particles: Origin, Emissions and Health Impacts. Nova Science Publisher, pp. 241-292.

Hedberg, Y., Gustafsson, J., Karlsson, H.L., Möller, L., Odnevall Wallinder, I., 2010. Bioaccessibility, bioavailability and toxicity of commercially relevant iron- and chromium-based particles: in vitro studies with an inhalation perspective. Particle and fibre toxicology 7, 23-23. (10.1186/1743-8977-7-23)

Hendryx, M., Luo, J., Chojenta, C., Byles, J.E., 2019. Air pollution exposures from multiple point sources and risk of incident chronic obstructive pulmonary disease (COPD) and asthma. Environ. Res. 179, 108783. (10.1016/j.envres.2019.108783)

Hernandez-Pellon, A., Nischkauer, W., Limbeck, A., Fernandez-Olmo, I., 2018. Metal(loid) bioaccessibility and inhalation risk assessment: A comparison between an urban and an industrial area. Environ. Res. 165, 140-149. (10.1016/j.envres.2018.04.014)

Hleis, D., Fernández-Olmo, I., Ledoux, F., Kfoury, A., Courcot, L., Desmonts, T., Courcot, D., 2013. Chemical profile identification of fugitive and confined particle emissions from an integrated iron and steelmaking plant. J. Hazard. Mater. 250-251, 246-255. (10.1016/j.jhazmat.2013.01.080)

Janssen, N.A.H., Yang, A., Strak, M., Steenhof, M., Hellack, B., Gerlofs-Nijland, M.E., Kuhlbusch, T., Kelly, F., Harrison, R., Brunekreef, B., Hoek, G., Cassee, F., 2014. Oxidative potential of particulate matter collected at sites with different source characteristics. Sci. Total Environ. 472, 572-581. (http://dx.doi.org/10.1016/j.scitotenv.2013.11.099)

Jedynska, A., Hoek, G., Wang, M., Yang, A., Eeftens, M., Cyrys, J., Keuken, M., Ampe, C., Beelen, R., Cesaroni, G., Forastiere, F., Cirach, M., de Hoogh, K., De Nazelle, A., Nystad, W., Akhlaghi, H.M., Declercq, C., Stempfelet, M., Eriksen, K.T., Dimakopoulou, K., Lanki, T., Meliefste, K., Nieuwenhuijsen, M., Yli-Tuomi, T., Raaschou-Nielsen, O., Janssen, N.A.H., Brunekreef, B., Kooter, I.M., 2017. Spatial variations and development of land use regression models of oxidative potential in ten

European study areas. Atmos. Environ. 150, 24-32. (https://doi.org/10.1016/j.atmosenv.2016.11.029)
Jia, Y.Y., Wang, Q., Liu, T., 2017. Toxicity Research of PM(2.5) Compositions In Vitro. Int. J. Environ. Res. Public. Health 14, 232. (10.3390/ijerph14030232)
Jiang, H., Ahmed, C.M.S., Zhao, Z., Chen, J.Y., Zhang, H., Canchola, A., Lin, Y.H., 2020. Role of functional groups in reaction kinetics of dithiothreitol with secondary organic aerosols. Environ. Pollut. 263. (10.1016/j.envpol.2020.114402)
Jovanovic, M.V., Savic, J.Z., Salimi, F., Stevanovic, S., Brown, R.A., Jovasevic-Stojanovic, M., Manojlovic, D., Bartonova, A., Bottle, S., Ristovski, Z.D., 2019. Measurements of oxidative potential of particulate matter at belgrade tunnel; comparison of BPEAnit, DTT and DCFH assays. Int. J. Environ. Res. Public. Health 16. (10.3390/ijerph16244906)
Jung, C.-H., Wells, W.W., 1998. Spontaneous Conversion ofl-Dehydroascorbic Acid tol-Ascorbic Acid andl-Erythroascorbic Acid. Arch. Biochem. Biophys. 355, 9-14. (10.1006/abbi.1998.0713)
Kelly, F.J., Fussell, J.C., 2012. Size, source and chemical composition as determinants of toxicity attributable to ambient particulate matter. Atmos. Environ. 60, 504-526. (https://doi.org/10.1016/j.atmosenv.2012.06.039)
Kfoury, A., Ledoux, F., Roche, C., Delmaire, G., Roussel, G., Courcot, D., 2016. $PM_{2.5}$ source apportionment in a French urban coastal site under steelworks emission influences using Constrained Non-Negative Matrix Factorization receptor model. J. Environ. Sci. (China) 40, 114-128. (10.1016/j.jes.2015.10.025)
Kumagai, Y., Koide, S., Taguchi, K., Endo, A., Nakai, Y., Yoshikawa, T., Shimojo, N., 2002. Oxidation of Proximal Protein Sulfhydryls by Phenanthraquinone, a Component of Diesel Exhaust Particles. Chem. Res. Toxicol. 15, 483-489. (10.1021/tx0100993)
Lê, S., Josse, J., Husson, F., 2008. FactoMineR: An R Package for Multivariate Analysis. J. Stat. Softw. 25, 1-18. (10.18637/jss.v025.i01)
Ledoux, F., Courcot, L., Courcot, D., Aboukaïs, A., Puskaric, E., 2006. A summer and winter apportionment of particulate matter at urban and rural areas in Northern France. Atmos. Res. 82, 633-642. (http://dx.doi.org/10.1016/j.atmosres.2006.02.019)
Ledoux, F., Kfoury, A., Delmaire, G., Roussel, G., El Zein, A., Courcot, D., 2017. Contributions of local and regional anthropogenic sources of metals in $PM_{2.5}$ at an urban site in Northern France. Chemosphere 181, 713-724. (https://doi.org/10.1016/j.chemosphere.2017.04.128)
Ledoux, F., Roche, C., Cazier, F., Beaugard, C., Courcot, D., 2018. Influence of ship emissions on NO_x, SO_2, O_3 and PM concentrations in a North-Sea harbor in France. Journal of Environmental Sciences 71, 56-66. (https://doi.org/10.1016/j.jes.2018.03.030)
Lelieveld, J., Pozzer, A., Pöschl, U., Fnais, M., Haines, A., Münzel, T., 2020. Loss of life expectancy from air pollution compared to other risk factors: a worldwide perspective. Cardiovasc. Res. (10.1093/cvr/cvaa025)
Li, J., Sun, S., Tang, R., Qiu, H., Huang, Q., Mason, T.G., Tian, L., 2016. Major air pollutants and risk of COPD exacerbations: a systematic review and meta-analysis. Int. J. Chron. Obstruct. Pulmon. Dis. 11, 3079-3091. (10.2147/copd.s122282)
Li, N., Sioutas, C., Cho, A., Schmitz, D., Misra, C., Sempf, J., Wang, M., Oberley, T., Froines, J., Nel, A., 2003. Ultrafine particulate pollutants induce oxidative stress and mitochondrial damage. Environ. Health Perspect. 111, 455-460. (10.1289/ehp.6000)
Lin, M., Yu, J.Z., 2019. Effect of metal-organic interactions on the oxidative potential of mixtures of atmospheric humic-like substances and copper/manganese as investigated

by the dithiothreitol assay. Sci. Total Environ. 697, 134012. (https://doi.org/10.1016/j.scitotenv.2019.134012)
Lippmann, M., 2014. Toxicological and epidemiological studies of cardiovascular effects of ambient air fine particulate matter ($PM_{2.5}$) and its chemical components: Coherence and public health implications. Crit. Rev. Toxicol. 44, 299-347. (10.3109/10408444.2013.861796)
Ma, Y., Cheng, Y., Qiu, X., Cao, G., Fang, Y., Wang, J., Zhu, T., Yu, J., Hu, D., 2018. Sources and oxidative potential of water-soluble humic-like substances ($HULIS_{WS}$) in fine particulate matter ($PM_{2.5}$) in Beijing. Atmos. Chem. Phys. 18, 5607-5617. (https://doi.org/10.5194/acp-18-5607-2018)
Marques, M.R.C., Loebenberg, R., Almukainzi, M., 2011. Simulated Biological Fluids with Possible Application in Dissolution Testing. Dissolution Technology 18, 15-28. (10.14227/DT180311P15)
Massamba, V.K., Coppieters, Y., Mercier, G., Collart, P., Levêque, A., 2014. Particle pollution effects on the risk of cardiovascular diseases. Ann. Cardiol. Angeiol. 63, 40-47. (10.1016/j.ancard.2013.08.017)
Mudway, I.S., Stenfors, N., Duggan, S.T., Roxborough, H., Zielinski, H., Marklund, S.L., Blomberg, A., Frew, A.J., Sandström, T., Kelly, F.J., 2004. An in vitro and in vivo investigation of the effects of diesel exhaust on human airway lining fluid antioxidants. Arch. Biochem. Biophys. 423, 200-212. (10.1016/j.abb.2003.12.018)
Nel, A., 2005. Air Pollution-Related Illness: Effects of Particles. Science 308, 804.
Paraskevopoulou, D., Bougiatioti, A., Stavroulas, I., Fang, T., Lianou, M., Liakakou, E., Gerasopoulos, E., Weber, R., Nenes, A., Mihalopoulos, N., 2019. Yearlong variability of oxidative potential of particulate matter in an urban Mediterranean environment. Atmos. Environ. 206, 183-196. (https://doi.org/10.1016/j.atmosenv.2019.02.027)
Patel, A., Rastogi, N., 2018. Oxidative potential of ambient fine aerosol over a semi-urban site in the Indo-Gangetic Plain. Atmos. Environ. 175, 127-134. (10.1016/j.atmosenv.2017.12.004)
Pay, M.T., Jiménez-Guerrero, P., Baldasano, J.M., 2012. Assessing sensitivity regimes of secondary inorganic aerosol formation in Europe with the CALIOPE-EU modeling system. Atmos. Environ. 51, 146-164. (https://doi.org/10.1016/j.atmosenv.2012.01.027)
Pay, M.T., Piot, M., Jorba, O., Gassó, S., Gonçalves, M., Basart, S., Dabdub, D., Jiménez-Guerrero, P., Baldasano, J.M., 2010. A full year evaluation of the CALIOPE-EU air quality modeling system over Europe for 2004. Atmos. Environ. 44, 3322-3342. (https://doi.org/10.1016/j.atmosenv.2010.05.040)
Perrone, M.R., Bertoli, I., Romano, S., Russo, M., Rispoli, G., Pietrogrande, M.C., 2019. $PM_{2.5}$ and PM_{10} oxidative potential at a Central Mediterranean Site: Contrasts between dithiothreitol- and ascorbic acid-measured values in relation with particle size and chemical composition. Atmos. Environ. 210, 143-155. (10.1016/j.atmosenv.2019.04.047)
Pietrogrande, M.C., Bertoli, I., Manarini, F., Russo, M., 2019. Ascorbate assay as a measure of oxidative potential for ambient particles: Evidence for the importance of cell-free surrogate lung fluid composition. Atmos. Environ. 211, 103-112. (https://doi.org/10.1016/j.atmosenv.2019.05.012)
Pietrogrande, M.C., Dalpiaz, C., Dell'Anna, R., Lazzeri, P., Manarini, F., Visentin, M., Tonidandel, G., 2018. Chemical composition and oxidative potential of atmospheric coarse particles at an industrial and urban background site in the alpine region of northern Italy. Atmos. Environ. 191, 340-350. (10.1016/j.atmosenv.2018.08.022)
Raaschou-Nielsen, O., Andersen, Z.J., Beelen, R., Samoli, E., Stafoggia, M., Weinmayr, G., Hoffmann, B., Fischer, P., Nieuwenhuijsen, M.J., Brunekreef, B., Xun, W.W.,

827 Katsouyanni, K., Dimakopoulou, K., Sommar, J., Forsberg, B., Modig, L., Oudin, A.,
828 Oftedal, B., Schwarze, P.E., Nafstad, P., De Faire, U., Pedersen, N.L., Ostenson, C.G.,
829 Fratiglioni, L., Penell, J., Korek, M., Pershagen, G., Eriksen, K.T., Sorensen, M.,
830 Tjonneland, A., Ellermann, T., Eeftens, M., Peeters, P.H., Meliefste, K., Wang, M.,
831 Bueno-de-Mesquita, B., Key, T.J., de Hoogh, K., Concin, H., Nagel, G., Vilier, A.,
832 Grioni, S., Krogh, V., Tsai, M.Y., Ricceri, F., Sacerdote, C., Galassi, C., Migliore, E.,
833 Ranzi, A., Cesaroni, G., Badaloni, C., Forastiere, F., Tamayo, I., Amiano, P.,
834 Dorronsoro, M., Trichopoulou, A., Bamia, C., Vineis, P., Hoek, G., 2013. Air pollution
835 and lung cancer incidence in 17 European cohorts: prospective analyses from the
836 European Study of Cohorts for Air Pollution Effects (ESCAPE). Lancet Oncol. 14, 813-
837 822. (10.1016/S1470-2045(13)70279-1)
838 Rolph, G., Stein, A., Stunder, B., 2017. Real-time Environmental Applications and Display
839 sYstem: READY. Environ. Modell. Softw. 95, 210-228.
840 (https://doi.org/10.1016/j.envsoft.2017.06.025)
841 Sauvain, J.-J., Rossi, M.J., Riediker, M., 2013. Comparison of Three Acellular Tests for
842 Assessing the Oxidation Potential of Nanomaterials. Aerosol Sci. Technol. 47, 218-227.
843 (10.1080/02786826.2012.742951)
844 Sax, S.N., Zu, K., Goodman, J.E., 2013. Air pollution and lung cancer in Europe. Lancet
845 Oncol. 14, e439-e440. (10.1016/s1470-2045(13)70438-8)
846 Stein, A.F., Draxler, R.R., Rolph, G.D., Stunder, B.J.B., Cohen, M.D., Ngan, F., 2015.
847 NOAA's HYSPLIT Atmospheric Transport and Dispersion Modeling System. Bull.
848 Am. Meteorol. Soc. 96, 2059-2077. (10.1175/bams-d-14-00110.1)
849 Verma, V., Fang, T., Xu, L., Peltier, R.E., Russell, A.G., Ng, N.L., Weber, R.J., 2015.
850 Organic aerosols associated with the generation of reactive oxygen species (ROS) by
851 water-soluble PM2.5. Environ. Sci. Technol. 49, 4646-4656. (10.1021/es505577w)
852 Visentin, M., Pagnoni, A., Sarti, E., Pietrogrande, M.C., 2016. Urban $PM_{2.5}$ oxidative
853 potential: Importance of chemical species and comparison of two spectrophotometric
854 cell-free assays. Environ. Pollut. 219, 72-79.
855 (https://doi.org/10.1016/j.envpol.2016.09.047)
856 Vreeland, H., Weber, R., Bergin, M., Greenwald, R., Golan, R., Russell, A.G., Verma, V.,
857 Sarnat, J.A., 2017. Oxidative potential of $PM_{2.5}$ during Atlanta rush hour: Measurements
858 of in-vehicle dithiothreitol (DTT) activity. Atmos. Environ. 165, 169-178.
859 (10.1016/j.atmosenv.2017.06.044)
860 Waked, A., Bourin, A., Michoud, V., Perdrix, E., Alleman, L.Y., Sauvage, S., Delaunay, T.,
861 Vermeesch, S., Petit, J.-E., Riffault, V., 2018. Investigation of the geographical origins
862 of PM_{10} based on long, medium and short-range air mass back-trajectories impacting
863 Northern France during the period 2009–2013. Atmos. Environ. 193, 143-152.
864 (10.1016/j.atmosenv.2018.08.015)
865 Wang, J., Lin, X., Lu, L., Wu, Y., Zhang, H., Lv, Q., Liu, W., Zhang, Y., Zhuang, S., 2019.
866 Temporal variation of oxidative potential of water soluble components of ambient $PM_{2.5}$
867 measured by dithiothreitol (DTT) assay. Sci. Total Environ. 649, 969-978.
868 (10.1016/j.scitotenv.2018.08.375)
869 WHO, 2018. World Health Organization. Fact sheets Ambient (outdoor) air pollution.
870 https://www.who.int/news-room/fact-sheets/detail/ambient-(outdoor)-air-quality-and-
871 health accessed the 10th of june 2020.
872 Wragg, J., Klinck, B., 2007. The bioaccessibility of lead from Welsh mine waste using a
873 respiratory uptake test. J. Environ. Sci. Health Part A Toxic-Hazard. Subst. Environ.
874 Eng. 42, 1223-1231. (10.1080/10934520701436054)
875 Yang, A., Jedynska, A., Hellack, B., Kooter, I., Hoek, G., Brunekreef, B., Kuhlbusch, T.A.J.,
876 Cassee, F.R., Janssen, N.A.H., 2014. Measurement of the oxidative potential of $PM_{2.5}$

and its constituents: The effect of extraction solvent and filter type. Atmos. Environ. 83, 35-42. (https://doi.org/10.1016/j.atmosenv.2013.10.049)

Yu, S., Liu, W., Xu, Y., Yi, K., Zhou, M., Tao, S., Liu, W., 2019. Characteristics and oxidative potential of atmospheric $PM_{2.5}$ in Beijing: Source apportionment and seasonal variation. Sci. Total Environ. 650, 277-287. (10.1016/j.scitotenv.2018.09.021)

Zielinski, H., Mudway, I.S., Bérubé, K.A., Murphy, S., Richards, R., Kelly, F.J., 1999. Modeling the interactions of particulates with epithelial lining fluid antioxidants. Am. J. Physiol. Lung Cell. Mol. Physiol. 277, L719-726. (10.1152/ajplung.1999.277.4.L719)

List of figures:

List of tables

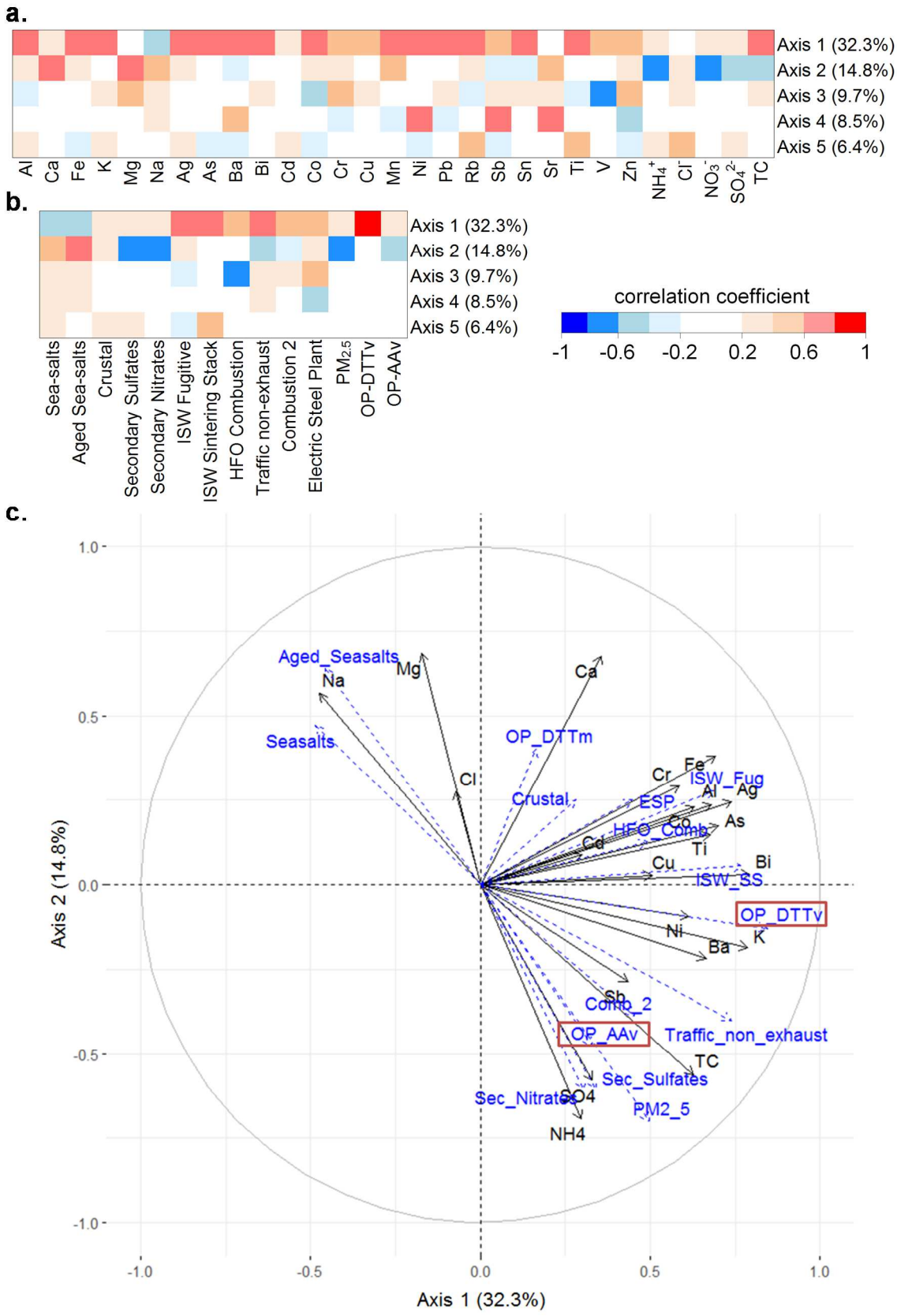
a.
Axis 1 (32.3%)
Axis 2 (14.8%)
Axis 3 (9.7%)
Axis 4 (8.5%)
Axis 5 (6.4%)
Al
Ca
Fe
K
Mg
Na
Ag
As
Ba
Bi
Cd
Co
Cr
Cu
Mn
Ni
Pb
Rb
Sb
Sn
Sr
Ti
V
Zn
NH4+
Cl-
NO3-
SO4 2-
TC
b.
Axis 1 (32.3%)
Axis 2 (14.8%)
Axis 3 (9.7%)
Axis 4 (8.5%)
Axis 5 (6.4%)
correlation coefficient
-1
-0.6
-0.2
0.2
0.6
1
Sea-salts
Aged Sea-salts
Crustal
Secondary Sulfates
Secondary Nitrates
ISW Fugitive
ISW Sintering Stack
HFO Combustion
Traffic non-exhaust
Combustion 2
Electric Steel Plant
PM2.5
OP-DTTv
OP-AAv
c.
Axis 2 (14.8%)
Axis 1 (32.3%)
1.0
0.5
0.0
-0.5
-1.0
Aged_Seasalts
Na
Mg
Ca
Seasalts
OP_DTTm
Cl
Crustal
Cr
Fe
ISW_Fug
Al
Ag
ESP
Co
As
HFO_Comb
Cd
Ti
Cu
Bi
ISW_SS
OP_DTTv
Ni
K
Ba
Sb
Comb_2
OP_AAv
Traffic_non_exhaust
TC
Sec_Sulfates
Sec_Nitrates
SO4
PM2_5
NH4

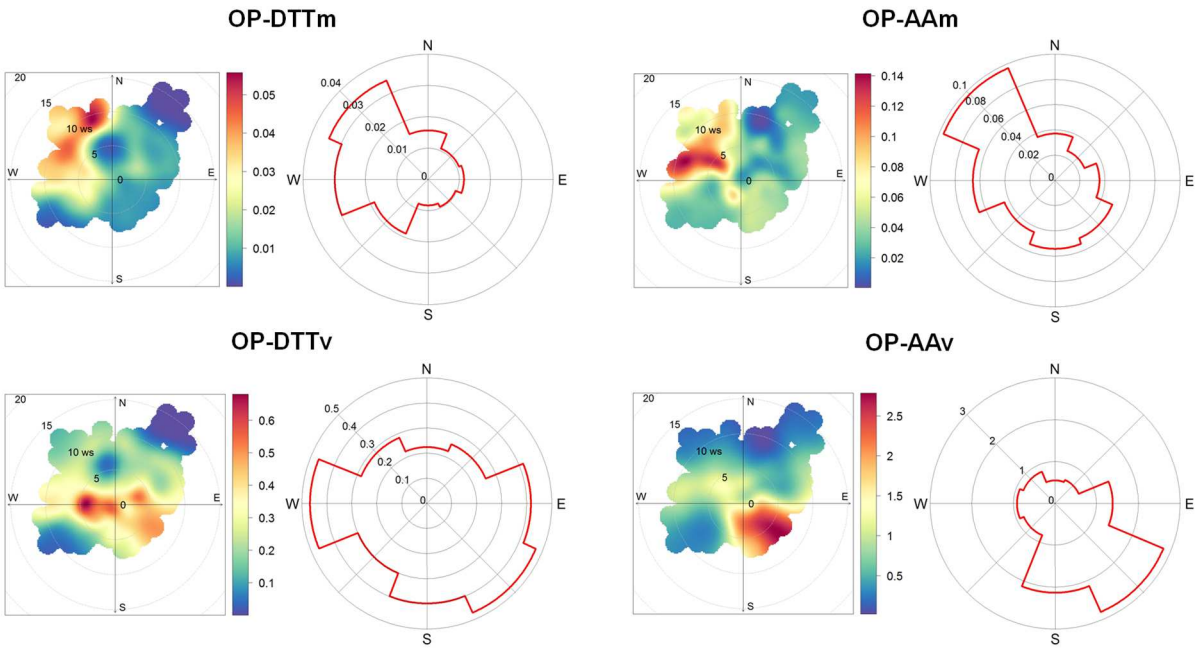
OP-DTTm
OP-AAm
OP-DTTv
OP-AAv
N
S
E
W
10 ws
20
15
5
0
0.04
0.03
0.02
0.01
0.05
0.14
0.12
0.1
0.08
0.06
0.6
0.5
0.4
0.3
0.2
2.5
2
1.5
1
0.5
3

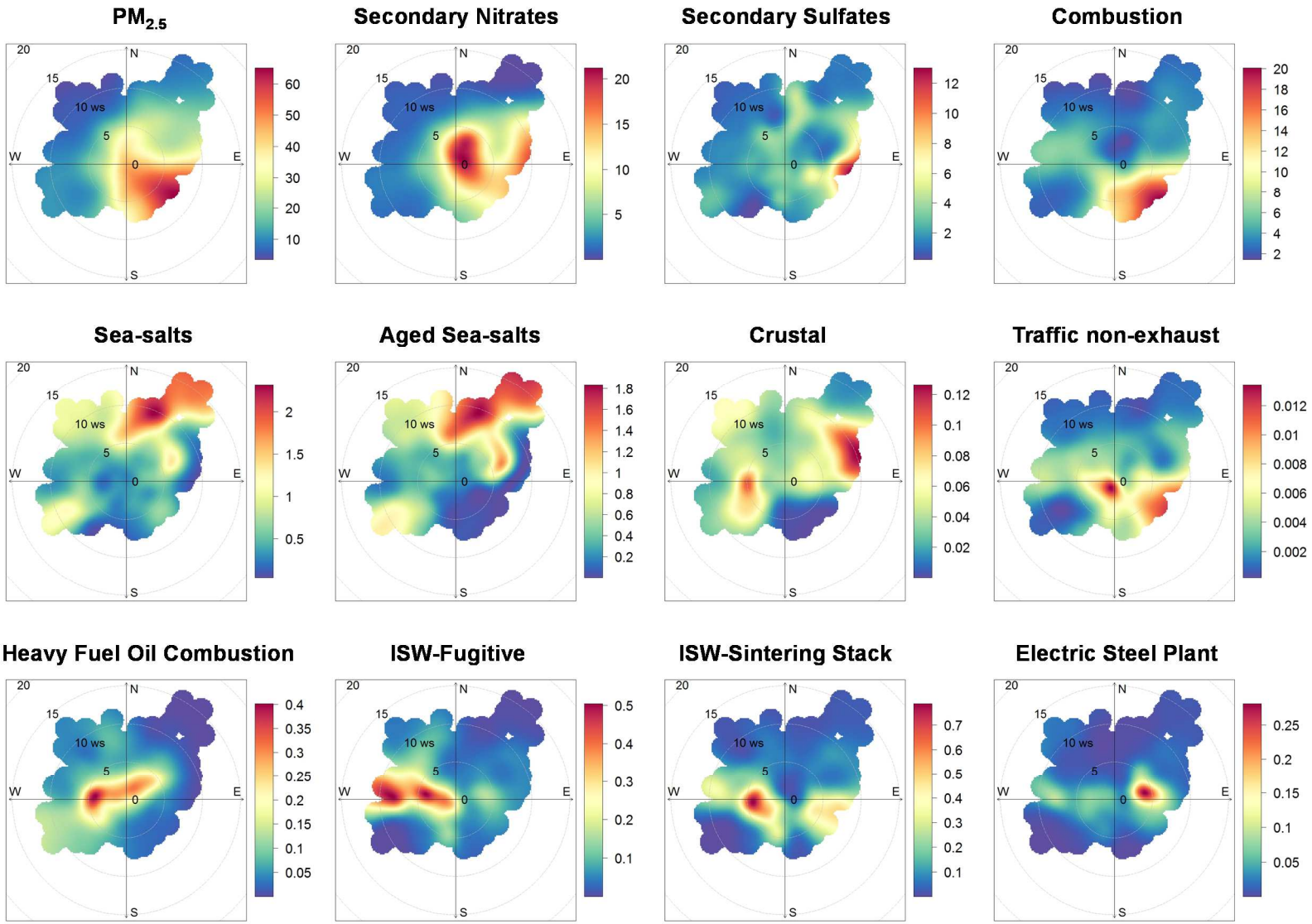
PM2.5
Secondary Nitrates
Secondary Sulfates
Combustion
Sea-salts
Aged Sea-salts
Crustal
Traffic non-exhaust
Heavy Fuel Oil Combustion
ISW-Fugitive
ISW-Sintering Stack
Electric Steel Plant
N
S
E
W
10 ws
5
15
20
0
60 50 40 30 20 10
20 15 10 5
12 10 8 6 4 2
20 18 16 14 12 10 8 6 4 2
2 1.5 1 0.5
1.8 1.6 1.4 1.2 1 0.8 0.6 0.4 0.2
0.12 0.1 0.08 0.06 0.04 0.02
0.012 0.01 0.008 0.006 0.004 0.002
0.4 0.35 0.3 0.25 0.2 0.15 0.1 0.05
0.5 0.4 0.3 0.2 0.1
0.7 0.6 0.5 0.4 0.3 0.2 0.1
0.25 0.2 0.15 0.1 0.05

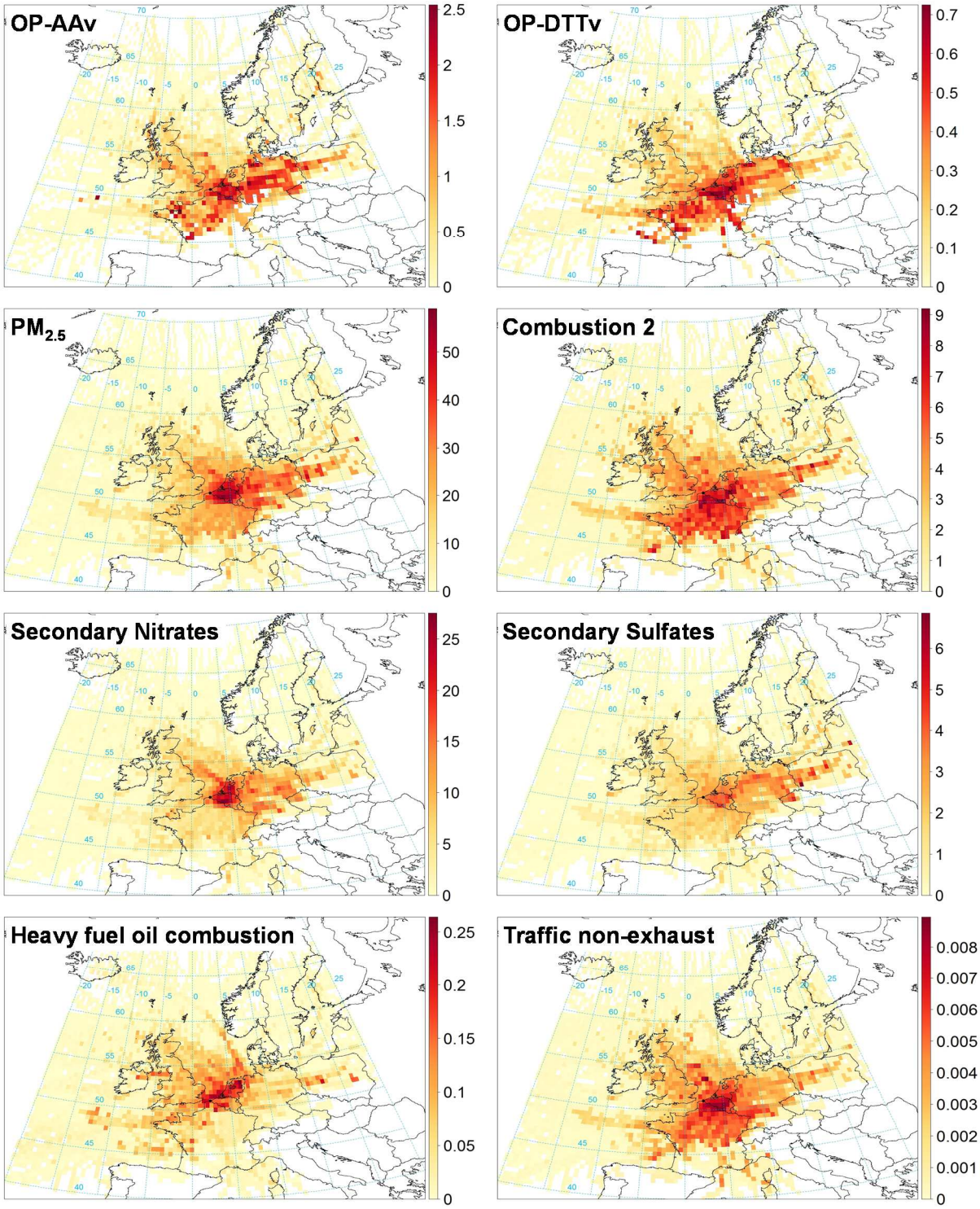
OP-AAv
2.5
2
1.5
1
0.5
0
OP-DTTv
0.7
0.6
0.5
0.4
0.3
0.2
0.1
0
PM2.5
50
40
30
20
10
0
Combustion 2
9
8
7
6
5
4
3
2
1
0
Secondary Nitrates
25
20
15
10
5
0
Secondary Sulfates
6
5
4
3
2
1
0
Heavy fuel oil combustion
0.25
0.2
0.15
0.1
0.05
0
Traffic non-exhaust
0.008
0.007
0.006
0.005
0.004
0.003
0.002
0.001
0

Species	Mean	Median	Min	Max	SD	1st Qu	3rd Qu
Al	26.5	22.5	2.52	112.2	18.7	14.8	30.7
Ca	76.2	62.7	19.4	286	48.2	43.7	88.4
Fe	155	84.0	9.1	1542	231	37.1	195
K	122.7	91.1	29.2	358	83.0	62.0	156
Mg	61.9	39.3	4.35	305	64.1	16.6	72.1
Na	372	225	21.1	2225	419	105	404
Ag	0.07	0.04	0.00	0.42	0.08	0.01	0.09
As	1.09	0.78	0.00	9.45	1.38	0.31	1.45
Ba	0.88	0.74	0.19	5.01	0.67	0.56	1.08
Bi	0.15	0.11	0.00	0.62	0.14	0.04	0.26
Cd	0.46	0.23	0.01	7.98	1.08	0.08	0.44
Co	0.18	0.12	0.02	0.9	0.17	0.07	0.25
Cr	1.36	0.79	0.07	9.88	1.55	0.52	1.61
Cu	3.13	1.63	0.17	31.0	4.46	0.81	4.25
Mn	13.7	4.84	0.12	92.4	20.7	1.59	14.3
Ni	5.36	3.23	0.73	41.55	6.35	1.91	6.29
Pb	14.8	8.26	0.75	118	18.4	3.95	18.8
Rb	0.57	0.43	0.05	4.86	0.73	0.19	0.57
Sb	1.05	0.63	0.00	15.0	2.05	0.37	1.10
Sn	1.03	0.80	0.08	5.43	0.98	0.28	1.33
Sr	0.49	0.40	0.16	1.87	0.32	0.30	0.59
Ti	2.00	1.10	0.00	15.2	2.66	0.29	2.47
V	5.16	3.13	0.49	23.1	5.31	1.84	5.84
Zn	67.6	26.4	1.96	625	113	8.38	88.5
NH_4^+	2010	1380	172	4817	1301	1043	3128
Cl^-	692	576	39.35	1752	409	418	841
NO_3^-	8678	3619	331	49066	10683	1837	11545
SO_4^{2-}	2754	2008	127	9642	2022	1399	3453
TC	5151	3612	805	17547	4246	2008	6881
$PM_{2.5}$ ($\mu g/m^3$)	29.2	18.8	3.1	90.8	24.4	11.30	44.30

Source	Markers (by order of abundance)	Contribution ($ng \cdot m^{-3}$)	
		Average ± SD	(min - max)
Sea-salts	Cl^-, Na, Mg	699 ± 605	(0 - 3000)
Aged Sea-salts	SO_4^{2-}, Na, NO_3^-, Mg, Cl^-	566 ± 595	(0 - 2166)
Crustal	Ca, Al, Fe, Mg, K	56 ± 55	(0 - 257)
Secondary Sulfates	SO_4^{2-}, NH_4^+	2645 ± 2313	(0 - 10985)
Secondary Nitrates	NO_3^-, NH_4^+	10294 ± 13601	(0 - 60318)
Heavy Fuel Oil Combustion	TC, V, Ni	145 ± 163	(0 - 620)
Combustion 2	TC, NH_4^+, NO_3^-, K	5444 ± 4312	(0 - 19352)
Traffic non-exhaust	Zn, Fe, Sb, Sn, Cr, Al, Pb, Mn, Cu	4.7 ± 4.3	(0 - 25)
ISW-Fugitive	Fe, Ca, Zn, Al, Mn, Pb, As	150 ± 204	(0 - 1296)
ISW-Sintering Stack	Cl^-, K, NH_4^+, Fe, Pb, Rb, Cd	209 ± 271	(0 - 1382)
Electric Steel Plant	Zn, Fe, Pb, Mg, Pb, Cr, Ca, Mn, Cu	77 ± 142	(0 - 746)

Site	Type	Leaching agent	OP-DDTv (nmol·min^{-1}·m^{-3})	OP-DTTm (pmol·min^{-1}·µg^{-1})	OP-AAv (nmol·min^{-1}·m^{-3})	OP-AAm (pmol·min^{-1}·µg^{-1})	$PM_{2.5}$ (µg·m^{-3})	PM_{10} (µg·m^{-3})	Reference
Dunkerque (FR)	urban industrial	G + Shk (24 h)	0.36	17.7	1.12	55	29.2		This study
Paris (FR)	urban	E + US (1 h)	0.23						(Jedynska et al., 2017)
Atlanta (USA)	urban	H_2O + US (30 min)	0.22	24					(Gao et al., 2020)
Hangzhou city (PRC)	urban	H_2O + US (30 min)	0.62	6.39			63.1		(Wang et al., 2019)
Beijing (PRC)	urban	H_2O + US (30 min)	12.6	130			113.8		(Yu et al., 2019)
Bologna (IT)	urban	PBS + US (15 min)	0.3-1.7		0.2-0.6				(Visentin et al., 2016)
Birmingham (USA)	urban	H_2O + US (30 min)			0.75				(Fang et al., 2016)
Grenoble (FR)	urban background	G + Shk (2 h)	1.00-4.12		0.17-2.46			7.4-22.3	(Calas et al., 2019)
Nice (FR)	urban background	G + Shk (2 h)	1.81-3.00		0.31-1.91			13.1-21.4	(Calas et al., 2019)
Talence (FR)	urban background	G + Shk (2 h)	1.08-2.97		0.21-1.59			8.7-26.2	(Calas et al., 2019)
Passy (FR)	urban background	G + Shk (2 h)	1.91-10.0		0.30-7.20			8.6-59.2	(Calas et al., 2019)
Sarno (IT)	urban background	H_2O + US (30 min)	0.19	11.67			16.3		(Cesari et al., 2019)
Lecce (IT)	urban background	H_2O + US (30 min)	0.29	18.4			16.8		(Chirizzi et al., 2017)
Trento (IT)	urban background	PBS + US (15 min)	0.58	50	0.7	50		19	(Pietrogrande et al., 2018)
Site in Netherlands	urban background	PBS + No Filt	1.4				17.3		(Janssen et al., 2014)
Athens (GR)	urban background	H_2O + US (30 min)	0.33	27.98					(Paraskevopoulou et al., 2019)
Salento (IT)	suburban	PBS + US (15 min)	0.19-0.29	10-11	0.09-0.21	5-8	20-26		(Perrone et al., 2019)
Patalia (IN)	semi-urban	M+H_2O + US (30 min)	3.8	27			150		(Patel and Rastogi, 2018)
Atlanta (USA)	side street	H_2O + US (30 min)	0.78	50			15.6		(Vreeland et al., 2017)
Belgrade (BU)	tunnel traffic	H_2O + Shk (90 min)	0.37	9.43					(Jovanovic et al., 2019)
Atlanta (USA)	highway	H_2O + US (30 min)	1.08	70			18.3		(Vreeland et al., 2017)
Ala (IT)	industrial (Zn)	PBS + US (15 min)	0.61	120	1.4	60		20.3	(Pietrogrande et al., 2018)

	OP-DTTv	OP-AAv		OP-DTTv	OP-AAv
Species			*Species*		
Al	**0.63***		V	0.47*	
Ca			Zn	**0.74***	0.49*
Fe	**0.77***	0.51*	NH_4^+	0.50*	*0.31*
K	0.67*	0.55*	Cl^-		
Mg	*-0.31*	-0.54*	NO_3^-	**0.68***	*0.39*
Na	-0.53*	**-0.62***	SO_4^{2-}	0.56*	*0.28*
Ag	**0.73***	0.52*	TC	**0.72***	**0.68***
As	**0.75***	**0.61***			
Ba	**0.79***	**0.69***	*Source contribution*		
Bi	**0.79***	*0.39*	Sea-salts	-0.40	*-0.39*
Cd	**0.82***	0.47*	Aged Sea-salts	-0.55*	**-0.67***
Co	**0.66***		Crustal		
Cr	**0.70***	0.56*	Secondary Sulfates	0.58*	*0.38*
Cu	**0.85***	**0.64***	Secondary Nitrates	**0.67***	*0.34*
Mn	**0.72***	*0.33*	HFO Combustion	0.45*	
Ni	**0.63***	*0.28*	Combustion 2	*0.37*	0.54*
Pb	**0.79***	**0.63***	Traffic non-exhaust	**0.80***	**0.66***
Rb	**0.75***	0.54*	ISW-Fugitive	**0.67***	0.46*
Sb	**0.70***	**0.60***	ISW-Sintering Stack	**0.60***	0.53*
Sn	**0.82***	**0.61***	Electric Steel Plant	**0.64***	0.43*
Sr		-0.45*			
Ti	**0.67***	*0.32*	*Oxidative potential*		
			OP-DTTv		0.46*
$PM_{2.5}$	**0.67***	0.45*	OP-AAv	0.46*	

$PM_{2.5}$ Oxidative Potential

Ascorbid Acid assay

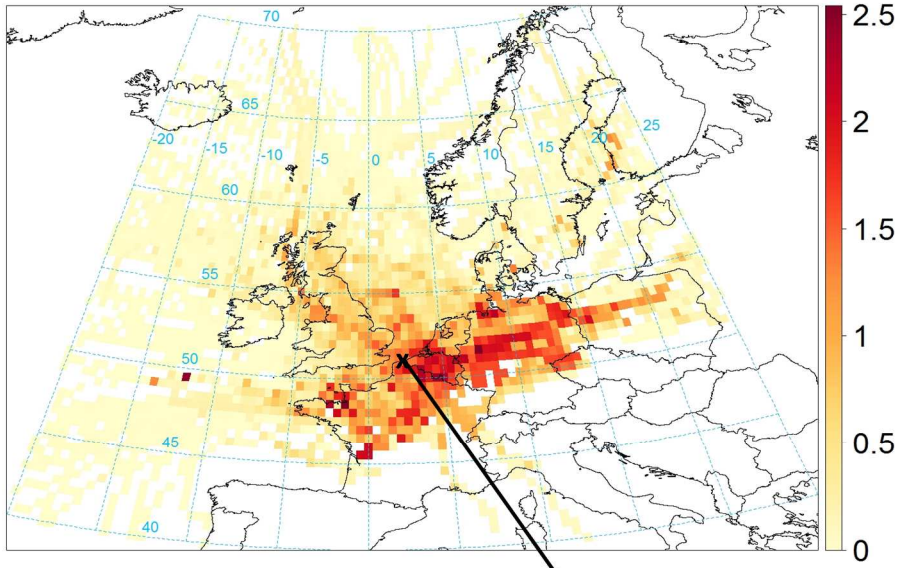

Related to:

Local and distant sources:
- Road traffic and biomass combustion

$PM_{2.5}$ concentration levels

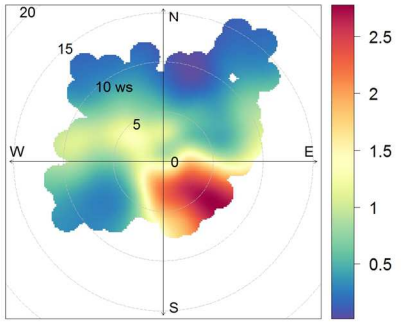

Dithiothreitol assay

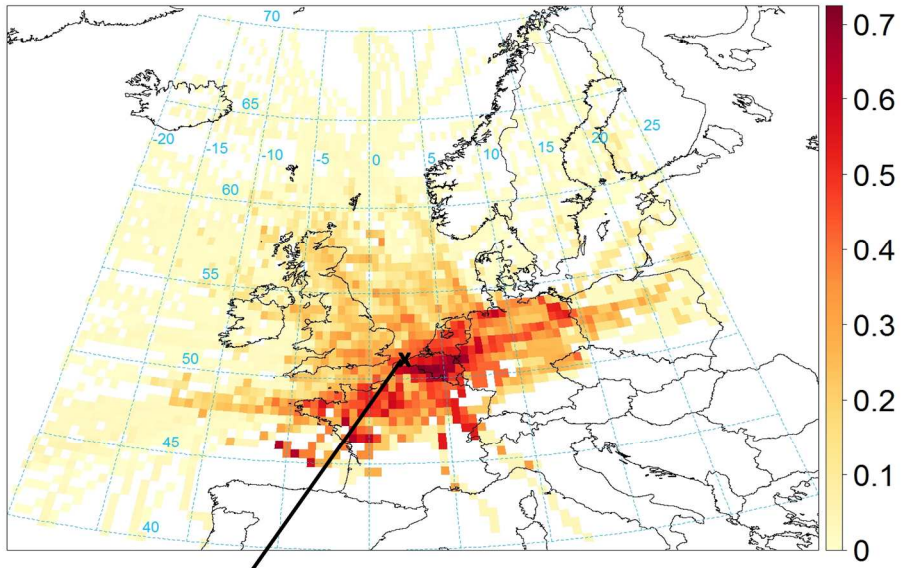

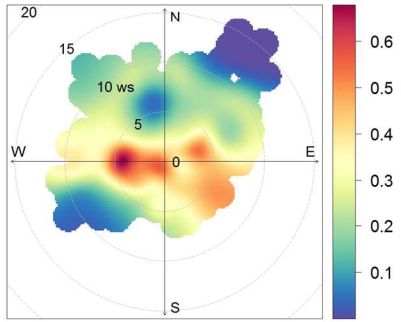

Related to:

Local industrial sources :
- Integrated steelworks
- Electric Steel Plant

Local and distant sources:
- Heavy fuel oil combustion
- Traffic non-exhaust
- Combustion possibly

No contribution of sea-salts, aged sea-salts, crustal sources, secondary sulfates and secondary nitrates to OP values